Photon Transitions in $\Upsilon(2S)$ and $\Upsilon(3S)$ Decays

M. Artuso,[1] C. Boulahouache,[1] S. Blusk,[1] J. Butt,[1] E. Dambasuren,[1] O. Dorjkhaidav,[1] J. Li,[1] N. Menaa,[1] R. Mountain,[1] H. Muramatsu,[1] R. Nandakumar,[1] R. Redjimi,[1] R. Sia,[1] T. Skwarnicki,[1] S. Stone,[1] J. C. Wang,[1] K. Zhang,[1] S. E. Csorna,[2] G. Bonvicini,[3] D. Cinabro,[3] M. Dubrovin,[3] A. Bornheim,[4] S. P. Pappas,[4] A. J. Weinstein,[4] J. L. Rosner,[5] R. A. Briere,[6] G. P. Chen,[6] T. Ferguson,[6] G. Tatishvili,[6] H. Vogel,[6] M. E. Watkins,[6] N. E. Adam,[7] J. P. Alexander,[7] K. Berkelman,[7] D. G. Cassel,[7] V. Crede,[7] J. E. Duboscq,[7] K. M. Ecklund,[7] R. Ehrlich,[7] L. Fields,[7] R. S. Galik,[7] L. Gibbons,[7] B. Gittelman,[7] R. Gray,[7] S. W. Gray,[7] D. L. Hartill,[7] B. K. Heltsley,[7] D. Hertz,[7] L. Hsu,[7] C. D. Jones,[7] J. Kandaswamy,[7] D. L. Kreinick,[7] V. E. Kuznetsov,[7] H. Mahlke-Krüger,[7] T. O. Meyer,[7] P. U. E. Onyisi,[7] J. R. Patterson,[7] D. Peterson,[7] J. Pivarski,[7] D. Riley,[7] A. Ryd,[7] A. J. Sadoff,[7] H. Schwarthoff,[7] M. R. Shepherd,[7] S. Stroiney,[7] W. M. Sun,[7] J. G. Thayer,[7] D. Urner,[7] T. Wilksen,[7] M. Weinberger,[7] S. B. Athar,[8] P. Avery,[8] L. Breva-Newell,[8] R. Patel,[8] V. Potlia,[8] H. Stoeck,[8] J. Yelton,[8] P. Rubin,[9] C. Cawlfield,[10] B. I. Eisenstein,[10] G. D. Gollin,[10] I. Karliner,[10] D. Kim,[10] N. Lowrey,[10] P. Naik,[10] C. Sedlack,[10] M. Selen,[10] J. J. Thaler,[10] J. Williams,[10] J. Wiss,[10] K. W. Edwards,[11] D. Besson,[12] T. K. Pedlar,[13] D. Cronin-Hennessy,[14] K. Y. Gao,[14] D. T. Gong,[14] Y. Kubota,[14] B. W. Lang,[14] S. Z. Li,[14] R. Poling,[14] A. W. Scott,[14] A. Smith,[14] C. J. Stepaniak,[14] S. Dobbs,[15] Z. Metreveli,[15] K. K. Seth,[15] A. Tomaradze,[15] P. Zweber,[15] J. Ernst,[16] A. H. Mahmood,[16] K. Arms,[17] K. K. Gan,[17] H. Severini,[18] D. M. Asner,[19] S. A. Dytman,[19] W. Love,[19] S. Mehrabyan,[19] J. A. Mueller,[19] V. Savinov,[19] Z. Li,[20] A. Lopez,[20] H. Mendez,[20] J. Ramirez,[20] G. S. Huang,[21] D. H. Miller,[21] V. Pavlunin,[21] B. Sanghi,[21] E. I. Shibata,[21] I. P. J. Shipsey,[21] G. S. Adams,[22] M. Chasse,[22] M. Cravey,[22] J. P. Cummings,[22] I. Danko,[22] J. Napolitano,[22] C. S. Park,[23] W. Park,[23] J. B. Thayer,[23] E. H. Thorndike,[23] T. E. Coan,[24] Y. S. Gao,[24] F. Liu,[24] and R. Stroynowski[24]

(CLEO Collaboration)

[1]*Syracuse University, Syracuse, New York 13244, USA*
[2]*Vanderbilt University, Nashville, Tennessee 37235, USA*
[3]*Wayne State University, Detroit, Michigan 48202, USA*
[4]*California Institute of Technology, Pasadena, California 91125, USA*
[5]*Enrico Fermi Institute, University of Chicago, Chicago, Illinois 60637, USA*
[6]*Carnegie Mellon University, Pittsburgh, Pennsylvania 15213, USA*
[7]*Cornell University, Ithaca, New York 14853, USA*
[8]*University of Florida, Gainesville, Florida 32611, USA*
[9]*George Mason University, Fairfax, Virginia 22030, USA*
[10]*University of Illinois, Urbana-Champaign, Illinois 61801, USA*
[11]*Carleton University, Ottawa, Ontario K1S 5B6, Canada and the Institute of Particle Physics, Canada*
[12]*University of Kansas, Lawrence, Kansas 66045, USA*
[13]*Luther College, Decorah, Iowa 52101, USA*
[14]*University of Minnesota, Minneapolis, Minnesota 55455, USA*
[15]*Northwestern University, Evanston, Illinois 60208, USA*
[16]*State University of New York at Albany, Albany, New York 12222, USA*
[17]*Ohio State University, Columbus, Ohio 43210, USA*
[18]*University of Oklahoma, Norman, Oklahoma 73019, USA*
[19]*University of Pittsburgh, Pittsburgh, Pennsylvania 15260, USA*
[20]*University of Puerto Rico, Mayaguez, Puerto Rico 00681, USA*
[21]*Purdue University, West Lafayette, Indiana 47907, USA*
[22]*Rensselaer Polytechnic Institute, Troy, New York 12180, USA*
[23]*University of Rochester, Rochester, New York 14627, USA*
[24]*Southern Methodist University, Dallas, Texas 75275, USA*

(Received 19 November 2004; published 25 January 2005)

We have studied the inclusive photon spectra in $\Upsilon(2S)$ and $\Upsilon(3S)$ decays using a large statistics data sample obtained with the CLEO III detector. We present the most precise measurements of electric dipole ($E1$) photon transition rates and photon energies for $\Upsilon(2S) \to \gamma\chi_{bJ}(1P)$ and $\Upsilon(3S) \to \gamma\chi_{bJ}(2P)$ ($J = 0, 1, 2$). We measure the rate for a rare $E1$ transition $\Upsilon(3S) \to \gamma\chi_{b0}(1P)$ for the first time. We also set upper limits on the rates for the hindered magnetic dipole ($M1$) transitions to the $\eta_b(1S)$ and $\eta_b(2S)$ states.

DOI: 10.1103/PhysRevLett.94.032001 PACS numbers: 14.40.Gx, 13.20.Gd

Long-lived $b\bar{b}$ states are especially well suited for testing lattice QCD calculations [1] and effective theories of strong interactions, such as potential models [2]. The narrow triplet-S states $\Upsilon(1S)$, $\Upsilon(2S)$, and $\Upsilon(3S)$ are directly formed in e^+e^- collisions. Six triplet-P states, $\chi_b(2P_J)$ and $\chi_b(1P_J)$ with $J = 2, 1, 0$, are reached via $E1$ photon transitions from the $\Upsilon(2S)$ and $\Upsilon(3S)$ states. Measurements of the photon energies determine the P-state masses, while measurements of the transition rates test theoretical predictions for $E1$ matrix elements. Such photon transitions were previously studied by CUSB [3], CUSB II [4], Crystal Ball [5], ARGUS [6], CLEO [7] and CLEO II [8] detectors. The CLEO III experiment accumulated 9.3×10^6 $\Upsilon(2S)$ and 5.9×10^6 $\Upsilon(3S)$ resonant decays, which constitute an order of magnitude increase in statistics over previous experiments. In this paper, we investigate inclusive photon spectra in decays of these resonances. In addition to the study of $E1$ photon transitions to P states, we also search for $M1$ photon transitions to yet unobserved singlet states, $\eta_b(1S)$ and $\eta_b(2S)$. A similar study of photon transitions in $\psi(2S)$ decays with the same detector has been recently reported elsewhere [9].

The CLEO III detector is equipped with a CsI(Tl) calorimeter, first installed in the CLEO II detector [10], with energy resolution matching that of the Crystal Ball [NaI(Tl) crystals] [5] and CUSB II (BGO crystals) detectors [4]. The finer segmentation of the CLEO calorimeter provides for better photon detection efficiency and more effective suppression of the photon background from π^0 decays than the previous experiments. The CLEO III tracking detector, consisting of a silicon strip detector and a large drift chamber [11], provides improved suppression of backgrounds from charged particles. The magnetic field inside the tracking detector was 1.5 T.

The data used in this analysis were collected at the Cornell Electron Storage Ring (CESR) at and near the $\Upsilon(1S)$, $\Upsilon(2S)$, and $\Upsilon(3S)$ resonances. The $\Upsilon(1S)$ data and the data taken at the continuum below each resonance are used for background subtraction as described below. Integrated luminosities accumulated on (off) resonance are 1.06 (0.19), 1.31 (0.44), and 1.39 (0.16) fb^{-1} for $\Upsilon(1S)$, $\Upsilon(2S)$, and $\Upsilon(3S)$, respectively.

The data analysis starts with the selection of hadronic events. We require that the observed number of charged tracks ($N_{\rm ch}$) be at least three. The visible energy of tracks and photons ($E_{\rm vis}$) must be at least 20% of the center-of-mass energy ($E_{\rm CM}$). For $3 \leq N_{\rm ch} \leq 4$ the total energy visible in the calorimeter alone ($E_{\rm cal}$) must be at least 15% of $E_{\rm CM}$ and, to suppress residual $e^+e^- \to e^+e^-(\gamma)$ events, the most energetic shower in the calorimeter must be less than 75% of the beam energy or $E_{\rm cal} < 0.85E_{\rm CM}$. The resulting event selection efficiency is 92% for decays of the $\Upsilon(nS)$ resonances.

To determine the number of produced resonant decays we subtract scaled continuum background from the number of hadronic events observed in the on-resonance data and correct for the selection efficiency. Cosmic-ray, beam-gas, and beam-wall backgrounds constitute less than a percent of the on-resonance data. They largely cancel in the subtraction of the off-resonance data. The systematic error on the number of resonant decays (2%) is dominated by uncertainty in Monte Carlo modeling of hadronic annihilation of the $b\bar{b}$ states.

In the next step of the data analysis we look for photon candidates in the selected hadronic events. Showers in the calorimeter are required not to match the projected trajectory of any charged particle, and to have a lateral shower profile consistent with that of an isolated electromagnetic shower. We restrict the photon candidates to be within the central barrel part of the calorimeter ($|\cos\theta| < 0.8$) where the photon energy resolution is optimal. The main photon background in this analysis comes from π^0 decays. We can reduce this background by removing photon candidates that combine with another photon to fit the π^0 mass. Unfortunately, this lowers the signal efficiency, since random photon combinations sometimes fall within the π^0 mass window. Our studies show that there is no benefit to applying the π^0 suppression for photon energies around 100 MeV where many of the dominant $E1$ photon lines are observed. This is in contrast with the recently analyzed $\psi(2S)$ decays [9] and is caused by the higher shower multiplicity in $b\bar{b}$ decays. The situation is different for

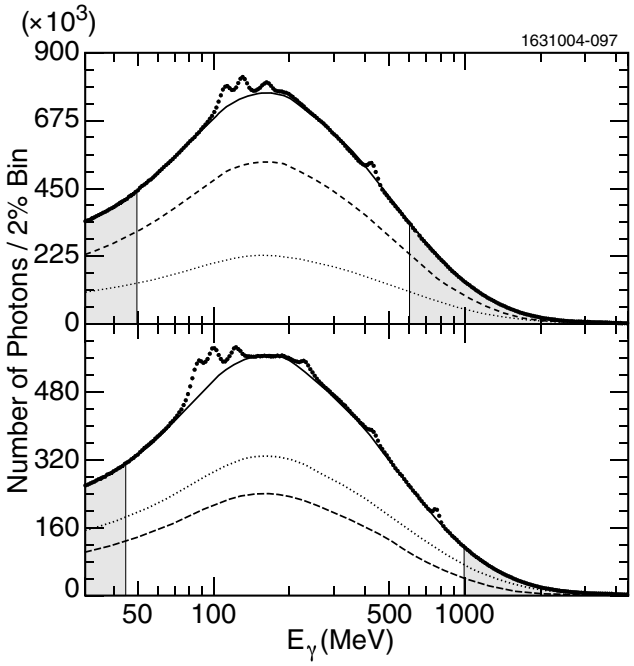

FIG. 1. Fit of the off resonance and $\Upsilon(1S)$ photon spectra to photon backgrounds in the $\Upsilon(2S)$ (top) and $\Upsilon(3S)$ (bottom) data. The energy regions used in the fit are shaded. The total fitted background is represented by the solid line. The $\Upsilon(2S)$ and $\Upsilon(3S)$ data are shown by points. The fitted contributions of the off resonance (dashed line) and $\Upsilon(1S)$ spectra (dotted line) are also shown. See the text for explanation of various photon lines observed in the data.

higher photon energies. Two photons in a decay of a fast π^0 must be spatially close to each other, which decreases the rate of false π^0 candidates. We suppress high energy photons, which match the π^0 mass when combined with another photon which satisfies $\cos\theta_{\gamma\gamma} > 0.7$, where $\theta_{\gamma\gamma}$ is the opening angle between the two photons.

Photon energy spectra obtained without π^0 suppression are shown for $\Upsilon(2S)$ and $\Upsilon(3S)$ decays in Fig. 1. Unlike in the $\psi(2S)$ photon spectrum, even dominant $E1$ peaks from $n^3S_1 \to (n-1)^3P_J$ transitions have a small signal-to-background ratio. This is not only due to the increased shower multiplicity but also to a significant continuum background in the on-resonance data. Furthermore, because the $b\bar{b}$ system is less relativistic, the three lines are more closely spaced due to the smaller fine-structure mass splitting. Therefore, estimation of the background level under the peaks is more challenging in this analysis. To constrain the background shape under the peaks we use the photon spectrum observed in the off-resonance data and in the $\Upsilon(1S)$ sample. The fraction of each is determined by a fit to the $\Upsilon(2S)$ or $\Upsilon(3S)$ photon spectra in the energy range free of any photon peaks. These regions are shown as shaded areas in Fig. 1. This procedure gives us a good approximation for the shape of these rapidly varying background components as illustrated in Fig. 1. Since photon backgrounds in decays of the χ_b states may deviate somewhat from the $\Upsilon(1S)$ photon spectrum, we allow for an additional, slowly varying background component, represented by a low order polynomial when fitting the peak region. The overall normalization of the continuum + $\Upsilon(1S)$ background is allowed to float in this fit. Systematic errors due to the background parametrization are evaluated by varying the fit ranges and the order of the polynomial.

The fits for $\Upsilon(2S) \to \gamma\chi_{bJ}(1P)$ and for $\Upsilon(3S) \to \gamma\chi_{bJ}(2P)$ photon lines are shown in Fig. 2 and Fig. 3, respectively. Since natural widths of the χ_b states are much smaller than the detector resolution, we represent each photon line as a Gaussian with an asymmetric low-energy tail induced by the transverse and longitudinal shower energy leakage out of the group of crystals used in the photon energy algorithm. This so-called Crystal Ball line shape is discussed in more detail elsewhere [9]. Shape parameters are varied to estimate systematic uncertainties. The widths of the Gaussian parts are constrained within the three lines to follow the energy dependence of the energy resolution predicted by Monte Carlo simulation. However, the absolute scale of the energy resolution is allowed to float in the fit. The fitted values of this scale factor are consistent between the $\Upsilon(2S)$, $\Upsilon(3S)$, and $\psi(2S)$ data.

The $\Upsilon(3S) \to \gamma\chi_{bJ}(2P)$ fit includes additional Doppler-broadened peaks due to $\Upsilon(2S) \to \gamma\chi_{bJ}(1P)$ and $\chi_{bJ}(2P) \to \gamma\Upsilon(1D)$. Parameters of these peaks are fixed in the fit from the other measurements and theoretical

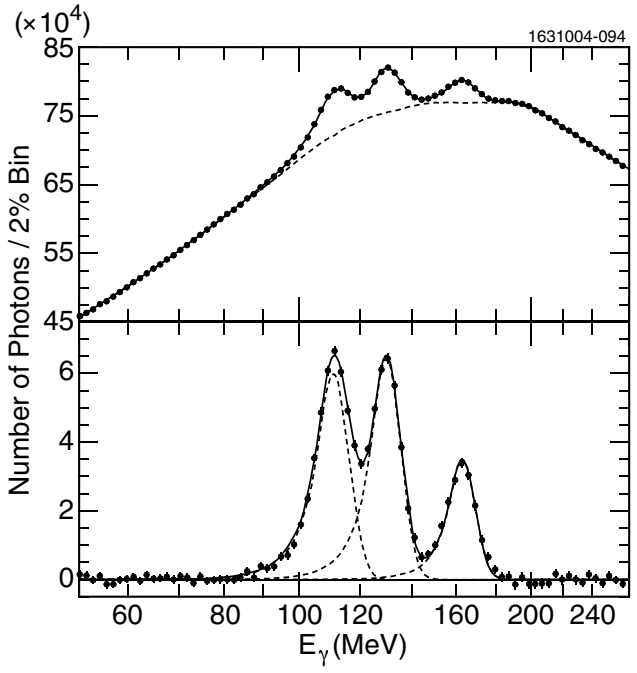

FIG. 2. Fit to the $\Upsilon(2S) \to \gamma\chi_{bJ}(1P)$ ($J = 2, 1, 0$) photon lines in the data. The points represent the data (top plot). Statistical errors on the data are smaller than the point size. The solid line represents the fit. The dashed line represents total fitted background. The background subtracted data (points with error bars) are shown at the bottom. The solid line represents the fitted photon lines together. The dashed lines show individual photon lines.

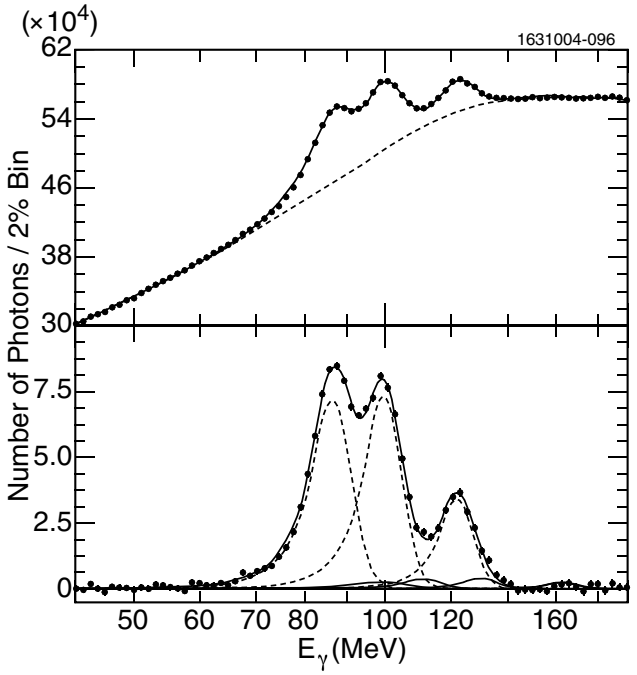

FIG. 3. Fit to the $\Upsilon(3S) \to \gamma\chi_{bJ}(2P)$ ($J = 2, 1, 0$) photon lines in the data. See caption of Fig. 2 for the description. Small solid line peaks in the bottom plot show the $\chi_{bJ}(2P) \to \gamma\Upsilon(1D)$ and $\Upsilon(2S) \to \gamma\chi_{bJ}(1P)$ contributions.

predictions [12]. The systematic errors include variations in the values of these parameters within the experimental and theoretical uncertainties. The obtained photon yields, selection efficiencies including proper photon angular distributions, determined branching ratios ($\mathcal{B}$), and peak energies are given in Table I. Since the statistical errors are very small, the results are dominated by the systematic uncertainties.

The largest systematic error in the E_γ measurements is due to the uncertainty in the absolute calibration of photon energies. This calibration error was improved over the one in the $\psi(2S) \to \gamma\chi_{cJ}(1P)$ photon energy measurements [9] by turning the latter results into recalibration points, given that the masses of the $\psi(2S)$ and $\chi_{cJ}(1P)$ states are known precisely from the scans of their resonant cross sections in e^+e^- and $\bar{p}p$ collisions [13]. The results for photon energies in transitions to the $\chi_{bJ}(1P)$ and $\chi_{bJ}(2P)$ states are in good agreement with previous measurements [3–8]. They are the most precise determinations. When combined with the measured masses of the $\Upsilon(2S)$ and $\Upsilon(3S)$ resonances, they allow for a determination of the masses of the χ_{bJ} states. A ratio of the fine mass splitting, $r \equiv (M(\chi_{b2}) - M(\chi_{b1}))/(M(\chi_{b1}) - M(\chi_{b0}))$, determined from our new photon energy measurements, gives very similar values for the $1P$ and $2P$ triplets: $0.574 \pm 0.005 \pm 0.011$ and $0.584 \pm 0.006 \pm 0.013$, respectively.

The branching ratio results for $\Upsilon(2S) \to \gamma\chi_{bJ}(1P)$ are also in good agreement with previous measurements [3,5–8], and offer improved experimental errors. However, the branching ratio results for $\Upsilon(3S) \to \gamma\chi_{bJ}(2P)$ are significantly larger than previous best measurements by CUSB II [4] based on photon samples which were about a factor of 50 smaller than utilized in this work.

In the nonrelativistic limit, branching ratios to different members of the same triplet differ only by the phase-space factors: $(2J + 1)E_\gamma^3$. We can test this prediction by calculating the ratio of the branching ratios, divided by the phase-space factors. The ratio $(J = 2)/(J = 1)$ is consistent with unity within the experimental errors: $1.009 \pm 0.016 \pm 0.077$ ($0.997 \pm 0.014 \pm 0.051$) for $1P$ ($2P$) states. However, the rate to the spin zero states appears to be lower: $0.822 \pm 0.020 \pm 0.063$ ($0.758 \pm 0.019 \pm 0.071$) for the $(J = 0)/(J = 1)$ $1P$ ($2P$) ratio and $0.814 \pm 0.020 \pm 0.112$ ($0.760 \pm 0.021 \pm 0.087$) for the $(J = 0)/(J = 2)$ $1P$ ($2P$) ratio. Suppression of the $J = 0$ matrix element was predicted by theoretical calculations implementing relativistic corrections [14,15].

The $\Upsilon(2S)$ photon spectrum in Fig. 1 shows a peak also at high energies (around 400 MeV) which is due to $\chi_{bJ}(1P) \to \gamma\Upsilon(1S)$ transitions. At these high energies our energy resolution is larger than the fine structure of these states, therefore the three peaks overlap each other. Systematic effects prevent us from reliably extracting individual line amplitudes. The similar cascade peaks, $\chi_{bJ}(2P) \to \gamma\Upsilon(2S)$ (around 250 MeV) and $\chi_{bJ}(2P) \to \gamma\Upsilon(1S)$ (around 800 MeV), are also seen in the $\Upsilon(3S)$ spectrum (Fig. 1).

The intermediate high energy peak in the $\Upsilon(3S)$ spectrum (around 400 MeV) is due to the overlap of primary, but rare, $\Upsilon(3S) \to \gamma\chi_{bJ}(1P)$ transitions and cascades $\chi_{bJ}(1P) \to \gamma\Upsilon(1S)$. The latter are fed not only by the direct transitions from the $\Upsilon(3S)$ to the $\chi_{bJ}(1P)$ states, but also by photon or hadronic transitions via the $\Upsilon(2S)$ and $\Upsilon(1D_J)$ states. One line, $\Upsilon(3S) \to \gamma\chi_{b0}(1P)$, has a photon energy sufficiently different from the rest of them that its amplitude can be measured. Amplitudes of the other two lines in this triplet, $\Upsilon(3S) \to \gamma\chi_{b1,2}(1P)$, cannot be reliably determined as they overlap each other and the cascade lines. The photon spectrum with π^0 suppression is used for this portion of the analysis. The three amplitudes of the photon lines for the direct transitions, $\Upsilon(3S) \to \gamma\chi_{bJ}(1P)$ ($J = 0,1,2$), are free parameters in the fit. They also contribute to the amplitudes of the cascade lines, $\chi_{bJ}(1P) \to \gamma\Upsilon(1S)$. The other contributions to the latter peaks are fixed from the measured [for the $\Upsilon(2S)$ route] or predicted [12] [for the $\Upsilon(1D_J)$ route] branching ratios. All photon energies are fixed to the known masses of the states involved. The fit is displayed in Fig. 4. The number of observed $\Upsilon(3S) \to \gamma\chi_{b0}(1P)$ events is $8,700 \pm 1100$ with a selection efficiency of 49%. The corresponding branching ratio is $\mathcal{B}(\Upsilon(3S) \to \gamma\chi_{b0}(1P)) = (0.30 \pm 0.04 \pm 0.10)\%$. This is the first determination of this rate. While various potential model calculations roughly agree with each other and our results for the rates of $\Upsilon(2S) \to \gamma\chi_{bJ}(1P)$ and $\Upsilon(3S) \to \gamma\chi_{bJ}(2P)$ transitions, the predictions for the $\Upsilon(3S) \to \gamma\chi_{b0}(1P)$ rate vary substantially and most of them are inconsistent with our measurement, as illustrated by the following sample of theoretical predictions [16]: 0.006% [17], 0.05% [18], 0.12% [14], 0.13% [19], 0.21% [20], 0.56% [21] and 0.74% [22].

TABLE I. The results for $\Upsilon(2S) \to \gamma\chi_{bJ}(1P)$ and $\Upsilon(3S) \to \gamma\chi_{bJ}(2P)$ ($J = 0, 1, 2$) transitions. The first errors are statistical, the second systematic.

initial state		$\Upsilon(2S)$			$\Upsilon(3S)$	
final state	$\chi_{b0}(1P)$	$\chi_{b1}(1P)$	$\chi_{b2}(1P)$	$\chi_{b0}(2P)$	$\chi_{b1}(2P)$	$\chi_{b2}(2P)$
# of γ's (10^3)	198 ± 6	407 ± 7	410 ± 6	225 ± 7	537 ± 7	568 ± 6
Efficiency (%)	57	63	61	57	63	61
$\mathcal{B}$ (%)	$3.75 \pm 0.12 \pm 0.47$	$6.93 \pm 0.12 \pm 0.41$	$7.24 \pm 0.11 \pm 0.40$	$6.77 \pm 0.20 \pm 0.65$	$14.54 \pm 0.18 \pm 0.73$	$15.79 \pm 0.17 \pm 0.73$
E_γ (MeV)	$162.56 \pm 0.19 \pm 0.42$	$129.58 \pm 0.09 \pm 0.29$	$110.58 \pm 0.08 \pm 0.30$	$121.55 \pm 0.16 \pm 0.46$	$99.15 \pm 0.07 \pm 0.25$	$86.04 \pm 0.06 \pm 0.27$

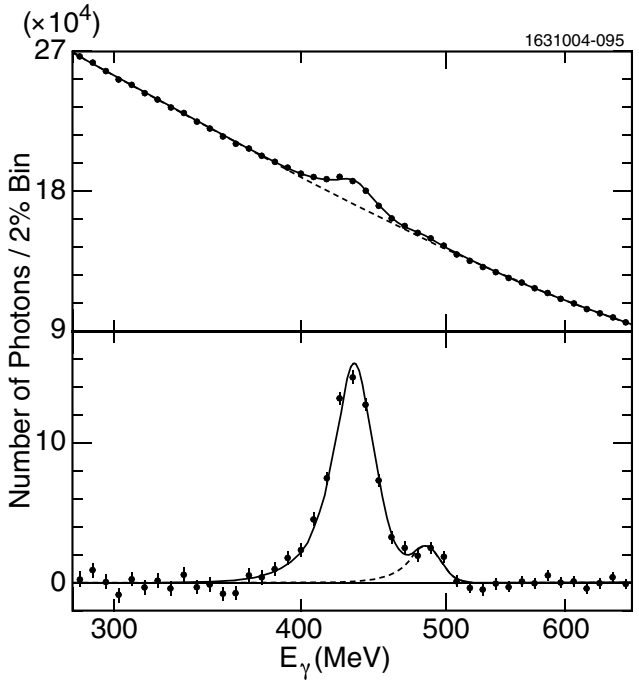

FIG. 4. Fit to six photon lines due to $\Upsilon(3S) \to \gamma\chi_{bJ}(1P)$ and $\chi_{bJ}(1P) \to \gamma\Upsilon(1S)$ ($J = 2, 1, 0$) in the data. See caption of Fig. 2 for the description. The dashed line in the bottom plot shows the $\Upsilon(3S) \to \gamma\chi_{b0}(1P)$ contribution by itself.

We have also analyzed our data for possible photon peaks due to hindered $M1$ transitions to singlet $\eta_b(1S)$ and $\eta_b(2S)$ states. Since the masses of these states are not known experimentally, we search for these transitions at photon energies corresponding to theoretical predictions [23]: $\eta_b(1S)$ ($\eta_b(2S)$) mass 35–110 (20–45) MeV below the $\Upsilon(1S)$ [$\Upsilon(2S)$] mass. No evidence for such transitions is found. We set the following 90% upper limits: $\mathcal{B}(\Upsilon(3S) \to \gamma\eta_b(1S)) < 4.3 \times 10^{-4}$, $\mathcal{B}(\Upsilon(3S) \to \gamma\eta_b(2S)) < 6.2 \times 10^{-4}$, and $\mathcal{B}(\Upsilon(2S) \to \gamma\eta_b(1S)) < 5.1 \times 10^{-4}$. These limits are a factor 5–7 lower than the branching ratio we measured for the hindered $M1$ transition in the $c\bar{c}$ system, $\psi(2S) \to \gamma\eta_c(1S)$ [9,24]. The limit on $\mathcal{B}(\Upsilon(3S) \to \gamma\eta_b(1S))$ appears to provide the tightest constraint on theoretical predictions, as illustrated by the following sample of theoretical predictions [16]: 29×10^{-4} [23,25], $(14–32) \times 10^{-4}$ [23,26], 5.2×10^{-4} [19] and 3.6×10^{-4} [22]. Only the last prediction is consistent with our upper limit.

In summary, we have reported improved photon energy and branching ratio measurements for the $E1$ transitions: $\Upsilon(2S) \to \gamma\chi_{bJ}(1P)$ and $\Upsilon(3S) \to \gamma\chi_{bJ}(2P)$ ($J = 0, 1, 2$). Our results are consistent with previous measurements, except for the branching ratios for the latter transitions which are found to be significantly higher. We have measured the rare $E1$ transition $\Upsilon(3S) \to \gamma\chi_{b0}(1P)$ for the first time. No evidence for hindered $M1$ transitions to $\eta_b(1S)$ and $\eta_b(2S)$ states is found in our data, against the expectations from some theoretical calculations.

We gratefully acknowledge the effort of the CESR staff in providing us with excellent luminosity and running conditions. This work was supported by the National Science Foundation and the U.S. Department of Energy.

[1] C. T. H. Davies *et al.*, Phys. Rev. Lett. **92**, 022001 (2004).
[2] For reviews see, e.g., D. Besson and T. Skwarnicki, Annu. Rev. Nucl. Part. Sci. **43**, 333 (1993); E. J. Eichten and C. Quigg, Phys. Rev. D **49**, 5845 (1994).
[3] CUSB, K. Han *et al.*, Phys. Rev. Lett. **49**, 1612 (1982); C. Klopfenstein *et al.*, Phys. Rev. Lett. **51**, 160 (1983).
[4] CUSB II, U. Heintz *et al.* Phys. Rev. D **46**, 1928 (1992).
[5] Crystal Ball, R. Nernst *et al.*, Phys. Rev. Lett. **54**, 2195 (1985).
[6] ARGUS, H. Albrecht *et al.*, Phys. Lett. B **160**, 331 (1985).
[7] CLEO, P. Haas *et al.*, Phys. Rev. Lett. **52**, 799 (1984).
[8] CLEO II, R. Morrison *et al.*, Phys. Rev. Lett. **67**, 1696 (1991); K. W. Edwards *et al.*, Phys. Rev. D **59**, 032003 (1999).
[9] CLEO III, S. B. Athar *et al.*, Phys. Rev. D **70**, 112002 (2004).
[10] CLEO II, Y. Kubota *et al.*, Nucl. Instrum. Methods Phys. Res., Sect. A **320**, 66 (1992).
[11] D. Peterson *et al.*, Nucl. Instrum. Methods Phys. Res., Sect. A **478**, 142 (2002).
[12] S. Godfrey and J. L. Rosner, Phys. Rev. D **64**, 097501 (2001); **66**, 059902(E) (2002); W. Kwong and J. L. Rosner, Phys. Rev. D **38**, 279 (1988).
[13] Particle Data Group, S. Eidelman *et al.*, Phys. Lett. B **592**, 1 (2004).
[14] P. Moxhay and J. L. Rosner, Phys. Rev. D **28**, 1132 (1983).
[15] R. McClary and N. Byers, Phys. Rev. D **28**, 1692 (1983).
[16] These theoretical predictions were rescaled to the recent value of the total width of the $\Upsilon(3S)$ resonance—see CLEO III, G. S. Adams *et al.*, Phys. Rev. Lett. **94** 012001 (2005).
[17] S. N. Gupta, S. F. Radford, and W. W. Repko, Phys. Rev. D **30**, 2424 (1984).
[18] L. P. Fulcher, Phys. Rev. D **42**, 2337 (1990).
[19] D. Ebert, R. Faustov, and V. Galkin, Phys. Rev. D **67**, 014027 (2003).
[20] F. Daghighian and D. Silverman, Phys. Rev. D **36**, 3401 (1987).
[21] H. Grotch, D. A. Owen, and K. J. Sebastian, Phys. Rev. D **30**, 1924 (1984).
[22] T. A. Lähde, Nucl. Phys. A **714**, 183 (2003).
[23] S. Godfrey and J. L. Rosner, Phys. Rev. D **64**, 074011 (2001); **65**, 039901(E) (2002) and references therein.
[24] Crystal Ball, J. E. Gaiser *et al.*, Phys. Rev. D **34**, 711 (1986).
[25] V. Zambetakis and N. Byers, Phys. Rev. D **28**, 2908 (1983).
[26] S. Godfrey and N. Isgur, Phys. Rev. D **32**, 189 (1985).